Turkish Journal of Electrical Engineering & Computer Sciences

http://journals.tubitak.gov.tr/elektrik/

Research Article

Turk J Elec Eng & Comp Sci
(2017) 25: 4398 – 4408

doi:10.3906/elk-1702-334

Design of adjustable T-shaped and Y-shaped photonic crystal power splitters for TM and TE polarizations

Mohammad DANAIE*, **Ruhallah NASIRIFAR**, **Abbas DIDEBAN**
Faculty of Electrical and Computer Engineering, Semnan University, Semnan, Iran

Received: 23.02.2017 • **Accepted/Published Online:** 06.06.2017 • **Final Version:** 05.10.2017

Abstract: In this paper, new topologies for realization of photonic crystal optical power splitters for TE and TM modes are proposed. The presented structures can be used for dividing input power with a desired ratio to output ports. The central input wavelength is designed for 1550 nm. To obtain wide-bandwidth power splitters for TE and TM modes, modified Y-shaped and T-shaped photonic crystal junctions are used. A triangular lattice of air holes and a square lattice of rods are used for Y-shaped and T-shaped platforms, respectively. For analyzing these structures, plane wave expansion and finite difference time domain methods are used. Simulation results show that the T-shaped splitter has a bandwidth equal to 51 nm, while the bandwidth of the Y-shaped structure is 126 nm. One of the advantages of the presented topologies is that the power share directed towards each output port can be determined by changing the radii of some specified rods and holes in their structures. For the designer to calculate the optimum radii of the holes based on his desired power ratio, some formulas are presented. Compared to the tunable power splitters based on directional couplers, this method provides much wider bandwidth and a more linear power ratio function.

Key words: Photonic crystals, power splitters, waveguides, T-junction, Y-branch

1. Introduction

Photonic crystals (PhCs) are dielectric material in which the refractive index changes periodically. They usually consist of materials with high and low refractive indices, which are arranged periodically in one, two, or three dimensions [1,2]. PhCs are among the many frameworks for implementing optical integrated circuits. Their unique feature is reflecting the light when its frequency is in the prohibited frequency region, which is referred to as the "photonic bandgap". Since the refractive index is a periodic function of the location, the behavior of a photon with specific frequency and energy depends on direction of its propagation in the structure. It gives PhCs unique features that can be utilized for designing a variety of optical devices. Applications of PhCs have been expanding over the past decades rapidly. They are used to design many optical devices such as switches, filters, and power splitter [1–3]. Among the main components in modern optical communication systems are power splitters. They can be used for directing the input optical signal towards the desired outputs. Power splitters can be implemented using directional couplers [4] or Y-shaped [5] and T-shaped junctions [6]. In recent years, many structures for realizing PhC power splitters have been suggested and designed [7–13]. A T-junction claimed to have significant transmission efficiency was designed in [8] based on coupled cavity waveguides. It has a high transmittance, but it does not use the standard W1 waveguides. Another power splitter structure was designed based on a photonic crystal slab in a silicon-on-insulator (SOI) material [9].

*Correspondence: danaie@semnan.ac.ir

This structure has two parallel outputs. It has high bandwidth and moderate splitting loss (less than 5% for each output). Another PhC splitter was presented in [10]. It uses a triangular array of holes etched into an InP/GaInAsP/InP heterostructure. The transmittance in this design is 75% but the curve of normalized power versus the wavelength is nonuniform.

For optical integrated circuits, splitters with nonequal power shares may also be needed. Wang et al. [11] designed magneto-optical and regular photonic crystals in a triangular lattice to create 1 $\times$ 2 and 1 $\times$ 3 beam splitters. The splitters can provide different amounts of powers in each output, but the transmittance of none of them is uniform versus the wavelength. Bagci et al. designed a T-shaped power splitter with a 60-nm bandwidth that has the transmittance efficiency of 90% and 75% for TE and TM polarizations, respectively [12]. Another design was presented for a T-shaped PhC optical power splitter with a flow control mechanism [13]. The authors added a central rod in the T-junction to change the output power share, but did not consider its effect on the reflectance.

In 2015, Mohammadi et al. [14] designed a compact integrated power splitting device with one output channel and two coupling areas. In their work, by using radius change and refractive index change in the coupling areas, a desired power splitting share could be achieved. The structure can be expanded to a 1 $\times$ N splitter. In the same year, Badaoui et al. [15] designed a 1 $\times$ 8 compact splitter with a 35-nm bandwidth and Huang et al. [16] presented a polarization beam splitter based on hybrid photonic crystal waveguide structures, where each output was for one of TM or TE polarized lights. A photonic crystal power splitter using ring resonators was designed in [17]. Ring resonators may provide high transmittance, but due to the existence of the resonator, they are narrow-band. Using wedge-like defects in the structure of a 120° Y-junction, a 1 $\times$ 3 power splitter was designed in [18]. It achieves a numerical transmittance of more than 99% for the central wavelength of 1550 nm; however, the sharp-angled wedge-type defects make the physical implementation difficult. In that design, the desired power splitting ratio was achieved by altering the wedge angle at the junction area of the power splitter. Consequently, wedge-type defects were also introduced in the structure of PhC bends [19,20] to improve their transmittance. Tee et al. also used this technique to design a cascaded 1 $\times$ 3 PhC power splitter based on asymmetric structural defects [21]. With the development of the idea of using PhCs to create power splitters, scientists have developed low-loss power splitters with different numbers of output. Some of these power splitters have 2 output ports [22–24], 3 output ports [18,25], and 4 output ports [26–28].

The study of power splitters shows that nearly all of them are designed in such a way that the transmitted power in each output be equal. Many have tried to change the number of output ports or obtain fixed output power ratios. Some have tried to increase the bandwidth or minimize the input reflection. In a few of these designs, such as in [18], different power ratios can be achieved for outputs. However, nonuniform transmittance through the wavelength is the problem of these designs. Based on the knowledge of the authors, no adjustable PhC power splitter with high bandwidth and constant power share versus wavelength has been proposed yet and we are trying to solve that problem. Compared to an electrical integrated circuit, in an all-optical photonic circuit, waveguides acts as wires that transmit the optical signal to different components. Each of these components may have different optical thresholds. If the designer needs to direct different shares of power to different components he has to have beam splitters with adjustable power shares. A good power splitter has to have a wide bandwidth and zero reflectance.

There are some major flaws in the structures presented in the literature. In most of them, the power share is 50% of the input power (they are not adjustable). They cannot direct an arbitrary percentage of the input power to the output ports. In a few of the topologies presented in the past, the adjustability capability exists, but

the disadvantage of those structures is their complexity. In other words, those structures are practically difficult to implement. The last challenge is that the power share should remain constant for different wavelengths. Obtaining a desired power ratio for a single wavelength is not very hard, but obtaining an adjustable ratio for a wide range of wavelength while keeping the reflectance minimum is quite challenging. In this paper, two new adjustable T-shaped and Y-shaped structures are presented. These structures are designed in such a way that the designer is able to achieve the intended power in each output. The structure suggested for this purpose is quite simple and practically not too complex for implementation.

The rest of the paper is organized as follows: in Section 2 we describe the numerical parameters and the simulation methods used for analyzing the structures. Section 3 explains the T-shaped topology designed for obtaining different power shares in the outputs. Section 4 is similarly devoted to the Y-junction. Simulation results and their interpretations are presented in Section 5 and the final section is devoted to the conclusions.

2. Numerical discussion

Different materials can be chosen for realizing optical devices. Since GaAs can also be used as a substrate for implementation of electronic circuits, here it is used as a substrate for creating PhC structures. These structures are designed for the commonly used fiber-optic communication wavelength of 1550 nm where the refractive index of GaAs is about 3.4. A photonic crystal slab with a triangular pattern of circular holes and a square lattice of rods (in air) are used for the Y-shaped and T-shaped power splitter structures, respectively. The Y-shaped PhC power splitter can be used for the TE polarization and the rod-type splitter is for TM polarization. Assuming that "a" is the lattice constant of the structure, we choose the radius of the holes in the triangular and square lattice to be 0.3a and 0.18a, respectively. The lattice constants of the structures are 430 nm and 645 nm for the hole-type and rod-type structures, respectively. The slab thickness of the triangular pattern is about 0.6a and the PhC is assumed to have air cladding [29,30]. For the rod-type structure, it is assumed that the rods are several times longer than the width of the input light beam so that a 2D approximation can be used. In order to analyze the structures, the plane wave expansion (PWE) method and finite difference time domain (FDTD) method are used to obtain the modal and time domain behavior of the PhC structures. In our FDTD simulations the mesh size is chosen as 1/16a, and simulations are performed for a 4-ps period of time, such that decreasing the mesh size or increasing the stop-time does not have a discernable effect on our simulation results. First, using the PWE method, the waveguide modes are calculated and the frequencies associated with them are obtained, and then in order to obtain the transmittance of each structure, an optical pulse with a Gaussian envelope is inserted to the beam splitter input ports. Using FDTD the electrical (E) and magnetic components of the electromagnetic fields are calculated at the output ports. The transmission and reflection spectra are obtained by integrating the Poynting vector "S", over a surface "A", normal to the waveguide path [31]. Assuming that P is the transmittance, we have Eq. (1):

$$\vec{P} = Re\left(\int_A \vec{S}.dA\right) \tag{1}$$

where the Poynting vector is defined as in Eq. 2:

$$\vec{S} = \frac{1}{2}\vec{E} \times \vec{H} \tag{2}$$

Hence, for each structure, the power directed to output ports and backward reflected powers are obtained. The Fourier transform of each output port is divided into the input incident spectrum to obtain the transmittance.

3. T-shaped power splitter

The quality of optical bends and junctions is very important when designing an adjustable PhC power splitter. High transmittance and low reflection are the most important requirements in these cases. To have an appropriate performance, PhC splitters must be designed to have the lowest reflected power. In the ideal case, zero reflection should exist for the maximum available wavelength range, namely the wavelength range associated with the input waveguides. To design the adjustable power splitter for TM modes, a two-dimensional (2D) square lattice of rods with refractive index of 3.4 embedded in air is used. Theoretically, these rods should be infinitely long to be considered as 2D PhCs. However, if they are several times longer than the incident beam width, they can be treated as 2D. Otherwise, they are usually fabricated as a slab, with a height nearly equal to 2a, where a is the lattice constant. In that case, they can use index guiding to confine the light in the vertical direction. Due to the difficulty of implementation, rod-type slab PhCs are not very popular. GaAs has a refractive index of 3.4 at the wavelength of 1550 nm. In order to maximize the optical bandgap, the radius of these rods is chosen as 0.18a, where a is equal to 644.8 nm. The suggested T-junction is shown in Figure 1 and the band diagram of the W1 waveguide used in the T-shaped power splitter is depicted in Figure 2. In this structure, rod radii are $r_1 = r_2 = r_3 = 0.077$a, $r_5 = 0.121$a, $r_6 = 0.142$a, and $r_4 = 0.225$a. As seen in Figure 1, this structure has one input and two outputs. In this structure, transmitted powers to each of outputs are equal to 49% of input power. Therefore, efficiency is very high and about 98% for the wavelength of 1550 nm. The bandwidth of the structure is from 1530 to 1685 nm. For the structure of Figure 1, the output ports receive similar portions of the input incident power.

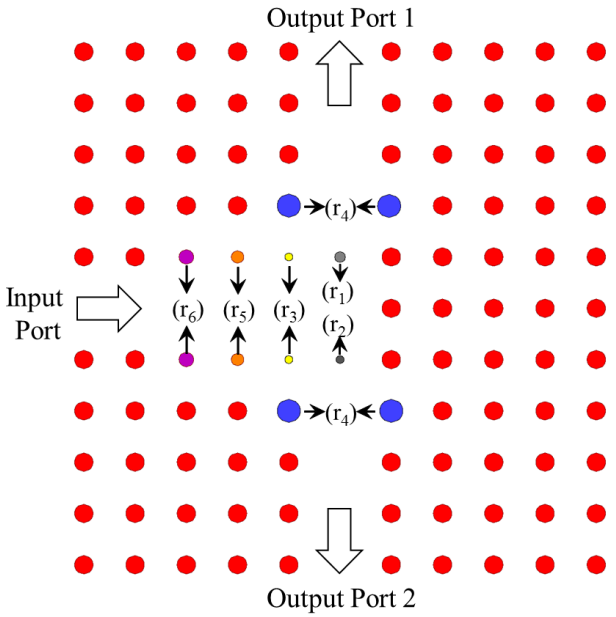

Figure 1. The T-shaped photonic crystal topology designed for TM polarized incident light.

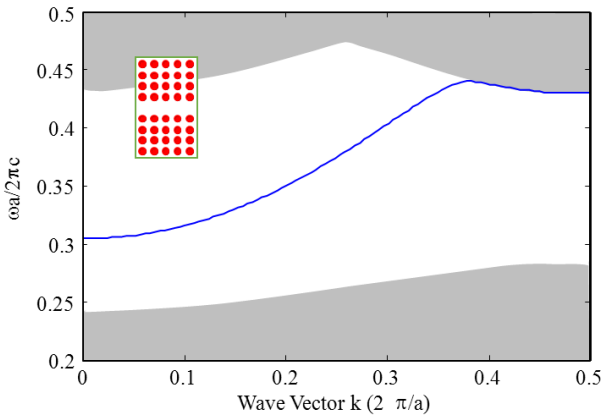

Figure 2. The band diagram of the W1 waveguide used in T-shaped power splitter obtained using PWE method.

In order to have adjustable power shares, one can use two methods. One of these methods is increasing radius r_1 while r_2 is constant, and the other one is decreasing r_2 while r_1 is constant. Figure 3 shows the variations of output power ratio in terms of variations of the ratio of r_1 to r_2. The results that are specified with dots are the FDTD simulations results when r_1 is increased and r_2 is constant. The stars are FDTD results when r_1 is constant and r_2 is decreased. According to Figure 3, exponential behavior for power ratio

is seen when the r_1 to r_2 ratio changes. Therefore, estimated equations can be obtained between r_1, r_2, and the power ratio to help designers in choosing their desired power share. To obtain an estimated formula, a function with the general form of y = Aexp(Bx) can be considered and then regression-based methods can be used to find A and B. These methods find the optimum values for those variables that minimize the root mean square (rms) error between the data and the formula-obtained values. MATLAB toolboxes support a variety of different equations and they can be used for this goal. Using only a single exponential function results in high rms error; therefore, the sum of two exponential functions is used to achieve an approximately 1% rms error. In the first method, r_2 is constant and r_1 increases. Eq. (3) shows the obtained approximate formula for this case. As seen in this case, if r_1 is increased and r_2 remains constant, a wider power ratio can be obtained. Furthermore, increasing r_2 will be much more practically convenient for fabrication than decreasing r_1.

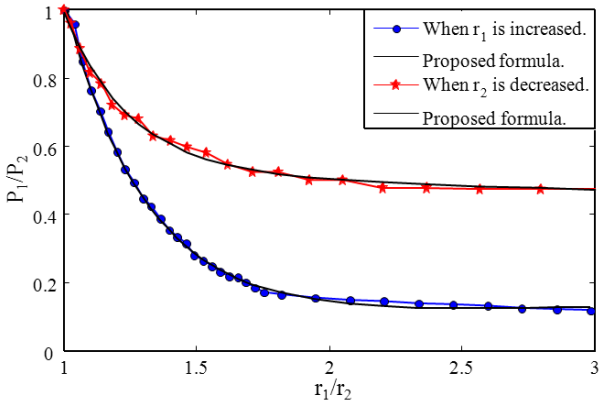

Figure 3. Diagram of power ratio in terms of variations of r_1 to r_2 ratio.

$$\frac{P_1}{P_2} = 25.12e^{-3.28\frac{r_1}{r_2}} + 0.078e^{0.164\frac{r_1}{r_2}} \tag{3}$$

Here, P_1 and P_2 are the optical powers of outputs 1 and 2 respectively. Since r_1 is constant, Eq. (3) can be approximated and simplified to:

$$Ln\left(\frac{P_1}{P_2}\right) = Ln\left(1.959e^{-40.467r_1}\right) \tag{4}$$

As a result, r_1 can be calculated according to Eq. (5). The root mean square error of Eq. (5) is 1.1%.

$$r_{1_{(P_1?P_2)}} = \frac{0.672 - Ln\left(\frac{P_1}{P_2}\right)}{40.467} \tag{5}$$

In the second method, r_1 is constant and r_2 decreases. The radius of r_2 to obtain the desired power is computable from Eq. (6).

$$\frac{P_1}{P_2} = 26.48e^{-4.026\frac{r_1}{r_2}} + 0.548e^{-0.051\frac{r_1}{r_2}} \tag{6}$$

Eq. (7) can be obtained by simplifying Eq. (6).

$$Ln\left(\frac{P_1}{P_2}\right) = Ln\left(14.42e^{\frac{-0.314}{a_2}}\right) \tag{7}$$

Finally, r_2 can be calculated according to Eq. (8). The root mean square error of Eq. (8) is 1.2%.

$$r_{2_{(P_1,P_2)}} = \frac{0.314}{2.66 - Ln\left(\frac{P_1}{P_2}\right)} \tag{8}$$

4. Y-shaped power splitter

Until 2003, most of the activities in the field of photonic crystal splitters were related to the 2D rod-type junctions. The major advantage of this system is creating a single-mode broadband waveguide by removing a row of dielectric rods. In these structures, light can pass through sharp bends and power splitting occurs easily. Unfortunately, though, implementation of rod-type PhCs is difficult. The PhC slab structure with a pattern of circular holes is easier for implementation and it is compatible with the integrated electronics fabrication technology. Unfortunately, the waveguide that is formed in this structure is not single-mode and it provides less bandwidth. It is obvious that a splitter made in this structure has to be Y-shaped. In this section, the Y-shaped power splitter is investigated and optimized. This proposed structure is shown in Figure 4. The band diagram of the W1 waveguide used in the Y-shaped power splitter is also shown in Figure 5. The blue section in this picture specifies the unacceptable leaky modes that are placed inside the light cone.

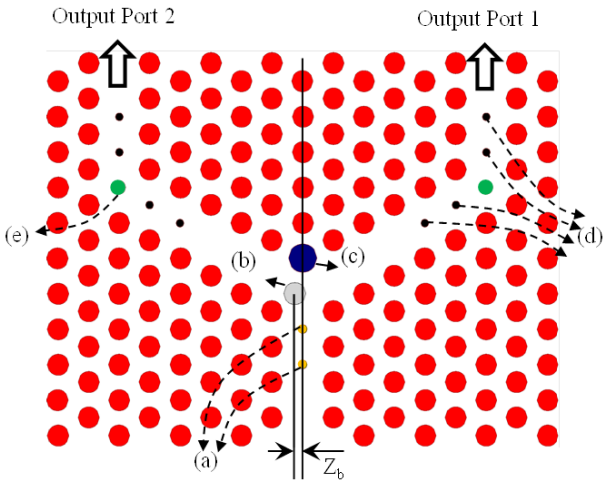

Figure 4. The Y-shaped photonic crystal topology designed for TE polarized incident light.

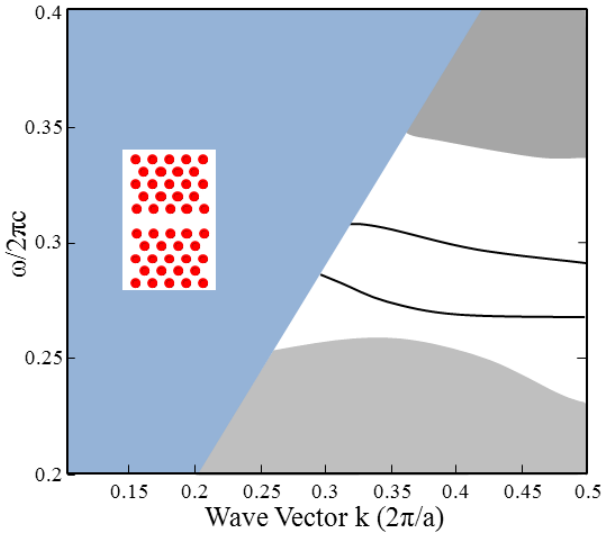

Figure 5. The band diagram of the W1 waveguide obtained using the PWE method.

The material used for this structure is the same as in the T-shaped splitter and the central wavelength is 1550 nm. Radii of the lattice holes are chosen as 0.3a and a is equal to 430 nm. The radii of modified holes are $r_a = 0.12$a, $r_b = 0.31$a, $r_c = 0.4$a, $r_e = 0.19$a, and $r_d = 0.11$a, which are obtained after optimization. As shown in Figure 4, Z_b is defined as the horizontal displacement of the central defect for the proposed Y-shaped splitter. If Z_b is equal to zero, this structure provides a bandwidth of more than 100 nm. Here, in order to obtain the desired power ratio in outputs, the coordinates of the "b" hole are altered. The transmitted power to outputs 1 and 2 will change by changing the coordinates of Z_b. The curve of outputs power ratio in terms of variations of Z_b is shown in Figure 6. According to Figure 6, it can be seen that there is an exponential equation between the outputs power ratio and Z_b. By calculating the proper Z_b, a desired power share will be directed to each output. Here Z_b is increased from 0 to 0.32a. Based on the obtained data, the required

coordinates of Z_b to obtain the desired power can be approximately computed from Eq. (9):

$$\frac{P_1}{P_2} = 0.473e^{(1.747?Z_b)} \tag{9}$$

where P_1 and P_2 are the light power of output 1 and output 2, respectively. Eq. (10) is obtained by simplifying Eq. (9):

$$Ln\left(\frac{P_1}{0.473}\right) = (1.747?Z_b) \tag{10}$$

Finally, Z_b can be calculated according to Eq. (11). The root mean square error of Eq. (11) is 1.2%.

$$Z_b = 0.428 + 0.572Ln\,(P_1) \tag{11}$$

5. Results and discussion

In this section, the effect of changing the tuning parameters on other aspects of power splitters such as bandwidth and backward reflection will be analyzed. First the rod-type structure is discussed and then hole-type PhC splitter will be scrutinized.

5.1. Effect of Increasing r_1

In this case, the radius of r_2 is constant. It is 0.077a, which is nearly equal to 50 nm. As shown in Figure 7, increasing r_1 will direct more power towards output 2. The total transmitted power is more than 90% and the reflected power is about 8%, as shown in

Figure 7. If r_1 and r_2 are equal, nearly 50% of input power is transmitted to each port. If r_1 is increased to 0.115a (75 nm), 20% is directed towards output 1 and 72% towards output 2 and 8% is reflected. The total transmitted power is more than 90% and loss power is less than 9% for r_1 between 50 nm and 75 nm. For larger values of r_1, the performance degrades and reflectance increases. Figure 8 shows the obtained transmittance versus wavelength for different amounts of r_1. It is very important that the transmittance remain flat, or group velocity dispersion will occur for the optical signal passing through the junction. As seen, the transmittance remains almost flat. The most important feature of our work is obtaining these flat curves. Otherwise, there

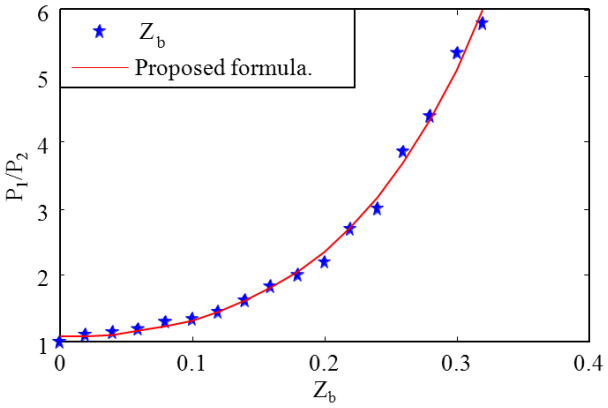

Figure 6. Diagram of power ratio in terms of variations of Z_b.

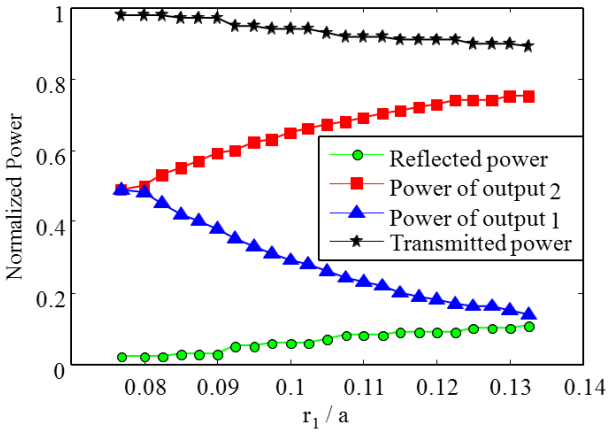

Figure 7. Variations of power in outputs, transfer power, and reflected power.

are much easier methods for having different power ratios, such as using PhC directional couplers. Directional couplers are narrowband, while our method provides a wideband transmittance. As shown in this figure, the bandwidth of power splitter in this method is about 160 nm.

Figure 9 shows the reflected power versus wavelength for different values or r_1. For most PhC junctions a reflectance of less than 10% is required. Except for $r_1 = 0.125$a, other values shown in Figure 9 satisfy that requirement.

5.2. Effect of decreasing r_2

For this case, the radius of r_1 is kept constant and it is 0.077a. The transmitted powers in output 1 and output 2 will decrease and increase with the reduction of r_2, respectively. The total transmitted power is about 98% and loss power is less than 2%, as shown in Figure 10. Overall, a better performance is observed in this case. However, it is more difficult in fabrication because it contains smaller features.

Figure 11 shows the bandwidth versus wavelength for five different values of r_2. As shown in this figure, the bandwidth of the power splitter in this method is about 100 nm and the curves are not as flat as before. Figure 12 shows the reflectance for the same values of r_2. The reflectance is nearly twice as good as in the previous case, but the problem is that the transmittance curves are not as flat as before. For the applications where group velocity dispersion is important, the first method is suggested, and if lower reflectance is needed, the second method may be used.

To sum up, according to the results of these two methods, the first one has more bandwidth but the reflected power in the second method is lower than in the first one. Therefore, these results show that increasing r_1 increases the bandwidth, and decreasing r_2 decreases the reflected power.

5.3. Effect of increasing Z_b

By changing the location of the "b" hole in Figure 4, the power share of outputs can be altered. The result is shown in Figure 13. For this method, the desired power share can be transferred to any outputs. According to the simulation results, almost 95% of the input power is transmitted to the output and 5% is returned to the input as a reflected power. The most important feature of this figure is that the power share change is linear, unlike the previous T-junction, which showed an almost exponential behavior. The second important feature is that it is a PhC slab, which is widely used and fabricated. We only change the coordinates of the hole, not

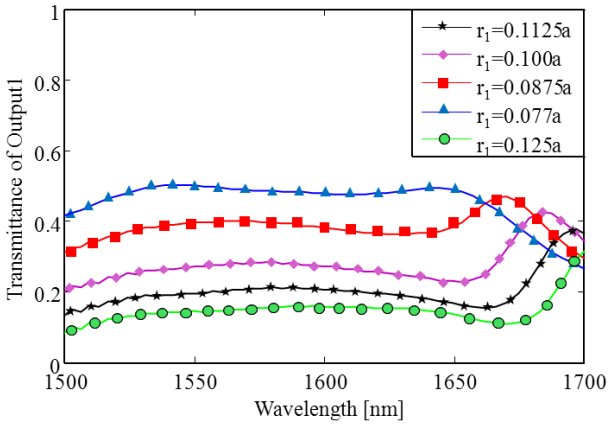

Figure 8. Power of output 1 and bandwidth.

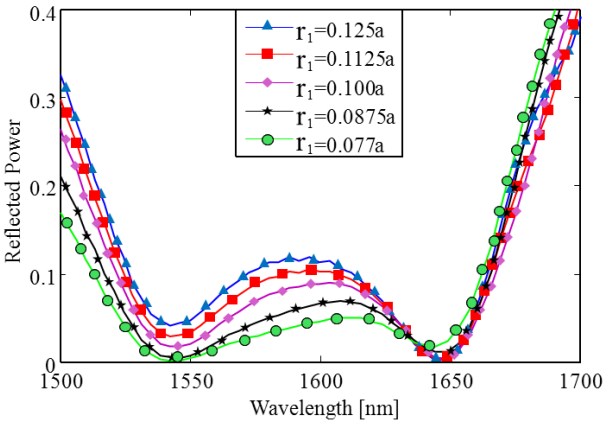

Figure 9. Reflected power when r_1 changes.

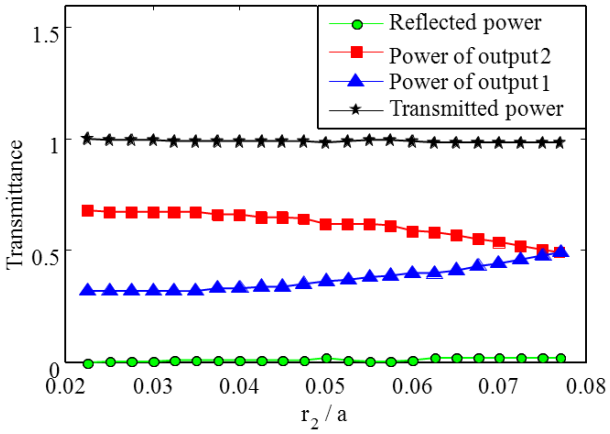

Figure 10. Variations of power in outputs, transfer power, and reflected power.

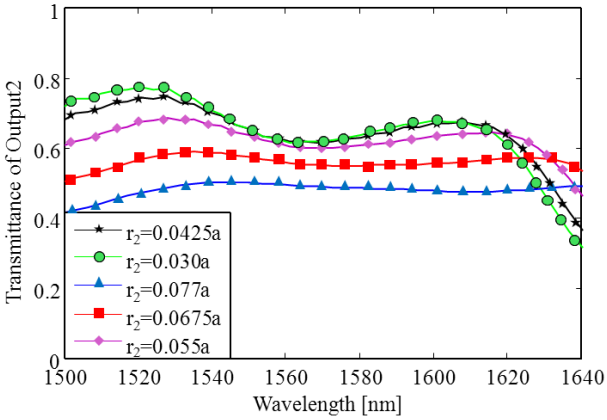

Figure 11. Power of output 2 and bandwidth.

its size, which is much easier for implementation and more robust against fabrication tolerance error. Figure 14 shows the power share of output 1 versus wavelength for different values of Z_b. As seen, nearly flat curves are obtained for bandwidth of more than 70 nm, which makes it applicable for many optical communication applications. Finally, the reflected power is shown in Figure 15. The reflected power remains less than 10% for nearly a 50-nm range.

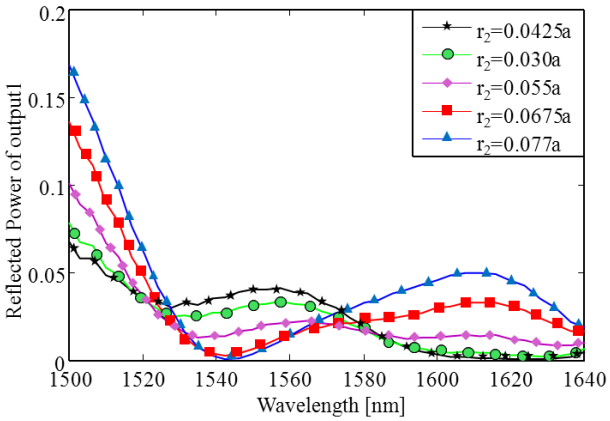

Figure 12. Reflected power for different values of r_2.

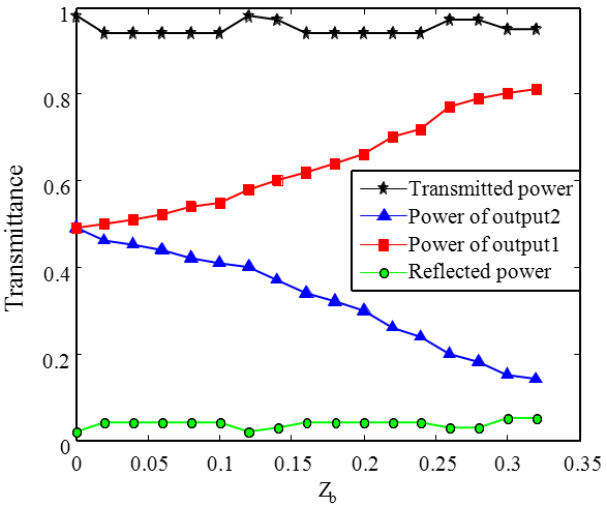

Figure 13. Variations of power in outputs, transmitted power, and reflected power.

6. Conclusions

Two Y-shaped and T-shaped photonic crystal optical power splitters were presented in this paper for TE and TM modes, respectively. The main advantage of these splitters is that the designer is able to achieve the intended power in each output port. Based on the knowledge of the authors, no adjustable PhC power splitter with a high bandwidth and constant power share versus wavelength has been proposed yet. The power dividers are designed to operate at the optical communication wavelength of 1550 nm. Approximate design formulas are presented for this reason. In terms of complexity, the structures do not use complicated or complex features.

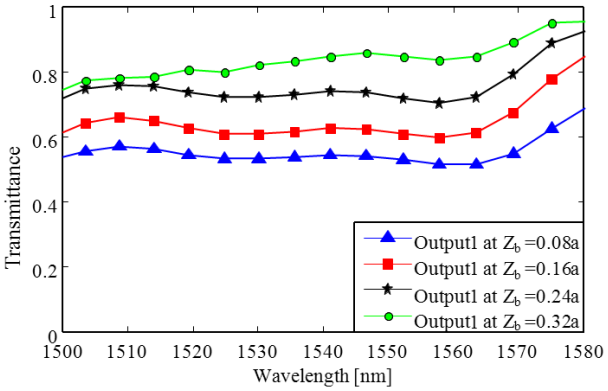

Figure 14. Power of output 1 and bandwidth.

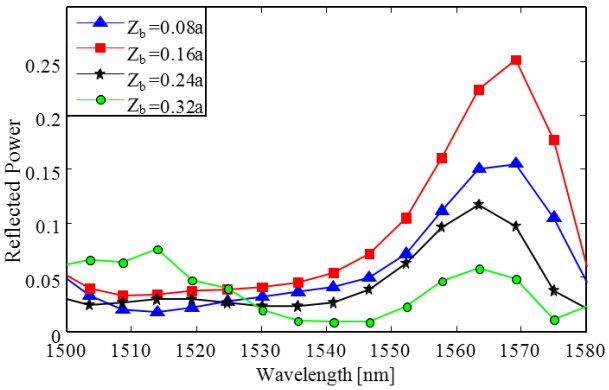

Figure 15. Reflected power for different values of Z_b.

The designers can achieve their desired power ratio only by changing the radii of some PhC defects or by changing their location. To analyze the structures, FDTD and PWE methods were used. Based on simulation results, the bandwidth of the T-shaped splitter was equal to 51 nm and the bandwidth of the Y-shaped structure was 126 nm. A reflectance of less than 10% was obtained in each case, which makes it applicable for many integrated optical devices.

References

[1] Joannopoulos JD, Johnson SG, Winn JN, Meade RD. Photonic Crystals: Molding the Flow of Light. 2nd ed. Princeton, NJ, USA: Princeton University Press, 2011.

[2] Gong Q, Hu X. Photonic Crystals: Principles and Applications. Boca Raton, FL, USA: Pan Stanford Publishing, 2014.

[3] Ghaffari A, Monifi F, Djavid M, Abrishamian MS. Photonic crystal bends and power splitters based on ring resonators. Opt Commun 2008; 281: 5929-5934.

[4] Park I, Lee HS, Kim HJ, Moon KM, Lee SG, Beom-Hoan O, Park SG, Lee EH. Photonic crystal power-splitter based on directional coupling. Opt Express 2004; 12: 3599-3604.

[5] Fan S, Johnson SG, Joannopoulos JD, Manolatou C, Haus HA. Waveguide branches in photonic crystals. J Opt Soc Am B 2001; 18: 162-165.

[6] Zhang Y, Li Z, Li B. Multimode interference effect and self-imaging principle in two-dimensional silicon photonic crystal waveguides for terahertz waves. Opt Express 2006; 14: 2679-2689.

[7] Hou Y, Fan F, Wang XH, Chang SJ. Terahertz power splitter based on ferrite photonic crystal. Optik 2013; 124: 5285-5288.

[8] Xu Q, Xie K, Ran Y, Tang J. 3dB power splitter design based on coupled cavity waveguides. Optik 2011; 122: 156-158.

[9] Yang D, Tian H, Ji Y. High-bandwidth and low-loss photonic crystal power-splitter with parallel output based on the integration of Y-junction and waveguide bends. Opt Commun 2012; 285: 3752-3757.

[10] Badaoui HA, Feham M, Abri M. Double bends and Y-shaped splitter design for integrated optics. Prog Electromag Res Lett 2012; 28: 129-138.

[11] Wang Z, Shen L, Yu Z, Zhang X, Zheng X. Highly efficient photonic-crystal splitters based on one-way waveguiding. J Opt Soc Am B 2013; 30: 173-176.

[12] Bagci F, Can S, Akaoglu B, Yilmaz AE. Polarization beam splitter based on self-collimation of a hybrid photonic crystal. Radio Eng 2014; 23: 1033-1037.

[13] Ahmed A, Robin H, Rokibul M, Goni MO. A novel approach to design photonic crystal based optical power splitter with a flow control mechanism. In: IEEE 2014 Electrical and Computer Engineering Conference; 20–22 December 2014; Dhaka, Bangladesh. New York, NY, USA: IEEE. pp. 493-495.

[14] Mohammadi M, Mansouri-Birjandi MA. Five-port power splitter based on pillar photonic crystal. IJST-T Electr Eng 2015; 39: 93-100.

[15] Badaoui HA, Abri M. Optimized 1×8 compact splitter based on photonic crystal using the two-dimensional finite-difference time-domain technique. Opt Eng 2015; 54: 067104.

[16] Huang Z, Yang X, Wang Y, Meng X, Fan R, Wang L. Ultrahigh extinction ratio of polarization beam splitter based on hybrid photonic crystal waveguide structures. Opt Commun 2015; 354: 9-13.

[17] Wu L, Wang M. Transmission performance of 1×2 type photonic crystal power splitter with ring resonators. Optik 2015; 126: 3613-3615.

[18] Tee DC, Kambayashi T, Sandoghchi SR, Tamchek N, Adikan FR. Efficient, wide angle, structure tuned 1×3 photonic crystal power splitter at 1550 nm for triple play applications. J Lightwave Technol 2012; 30: 2818-2823.

[19] Tee DC, Shee YG, Tamchek N, Adikan FR. Structure tuned, high transmission 180 waveguide bend in 2-D planar photonic crystal. IEEE Photonic Tech L 2013; 25: 1443-1446.

[20] Tee DC, Tamchek N, Abu Bakar MH, Mahamd Adikan FR. High-transmission-efficiency 120° photonic crystal waveguide bend by using flexible structural defects. IEEE Photonics J 2014; 6: 1-10.

[21] Tee DC, Tamchek N, Shee YG, Adikan FM. Numerical investigation on cascaded 1×3 photonic crystal power splitter based on asymmetric and symmetric 1×2 photonic crystal splitters designed with flexible structural defects. Opt Express 2014; 22: 24241-24255.

[22] Yucel MB, Cicek A, Ulug B. Polarization-independent beam splitting by a photonic crystal right prism. Appl Phys B-Lasers O 2013; 113: 107-114.

[23] Sharma J, Sharma R, Dusad LK. Review and analysis of photonic crystal beam splitters for optical communication applications. In: IEEE 2015 Green Computing and Internet of Things Conference; 8–10 October 2015; Noida, India. New York, NY, USA: IEEE. pp. 160-162.

[24] Xu Y, Xiao J. An ultracompact polarization-insensitive silicon-based strip-to-slot power splitter. IEEE Photonic Tech L 2015; 28: 536-539.

[25] Wang H, He L. Highly efficient 1×3 power splitter at 1550 nm for triple play applications using photonic crystal waveguides. Opt Eng 2014; 53: 075104.

[26] Wang Z, Ning B. Compact, wide bandwidth, multi-channel power dividers based on one-dimensional photonic crystal waveguides. Optik 2014; 125:694-696.

[27] Zhou J, Tian H, Yang D, Liu Q, Huang L, Ji Y. Low-loss, efficient, wide-angle 1×4 power splitter at $\sim$1.55 μm wavelengths for four play applications built with a monolithic photonic crystal slab. Appl Optics 2014; 53: 8012-8019.

[28] Chen B, Liu C, Si J. Design of broadband power splitters using two-mode interference in slot waveguides. Opt Commun 2015; 355: 367-375.

[29] Foghani S, Kaatuzian H, Danaie M. Simulation and design of a wideband T-shaped photonic crystal splitter. Opt Appl 2010; 40: 863-872.

[30] Danaie M, Kaatuzian H. Bandwidth improvement for a photonic crystal optical Y-splitter. J Opt Soc Korea 2011; 15: 283-288.

[31] Moghaddami MK, Mirsalehi MM, Attari AR. A 60° photonic crystal waveguide bend with improved transmission characteristics. Opt Appl 2009; 39: 307-317.